SPECIAL REPORT

CNS Oncology

For reprint orders, please contact: reprints@futuremedicine.com

Radial expansion rates and tumor growth kinetics predict malignant transformation in contrast-enhancing low-grade diffuse astrocytoma

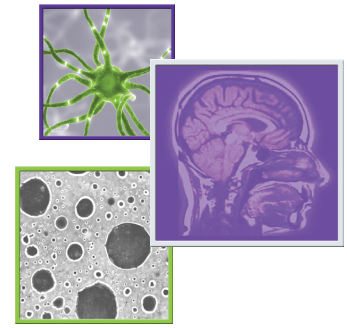

Leith Hathout[1], Whitney B Pope[2], Albert Lai[3,4], Phioanh L Nghiemphu[3,4], Timothy F Cloughesy[3,4] & Benjamin M Ellingson*[,2,3,5,6]

Practice points

- Contrast-enhancing low-grade diffuse astrocytomas are an understudied, aggressive subtype at increased risk because of few radiographic indications of malignant transformation.
- Clinicians currently use subjective assessments, not quantitative evaluations, to gain a sense of how fast the tumor is growing by examining serial MRIs.
- Quantitative volumetry and biomathematical modeling techniques may be useful for objectively evaluating whether tumor growth rates provide indications of malignant transformation.
- Consistent with previous studies, results suggest that tumors expanding rapidly or having higher proliferation rates estimated from mathematical models are more likely to have undergone malignant transformation compared with slower growing tumors.
- Results also suggest that simple measures of radial expansion may be both easier and more accurate in predicting malignant transformation compared with more sophisticated modeling techniques.

SUMMARY **Background:** Contrast-enhancing low-grade diffuse astrocytomas are an understudied, aggressive subtype at increased risk because of few radiographic indications of malignant transformation. In the current study, we tested whether tumor growth kinetics could identify tumors that undergo malignant transformation to higher grades. **Methods:** Thirty patients with untreated diffuse astrocytomas (WHO II) that underwent tumor progression were enrolled. Contrast-enhancing and T2 hyperintense tumor regions were segmented and the radius of tumor at two time points leading to progression was estimated. Radial expansion rates were used to estimate proliferation and invasion rates using a biomathematical model. **Results:** Radial expansion rates for both contrast-enhancing ($p = 0.0040$) and T2 hyperintense regions ($p = 0.0016$) were significantly higher in WHO II–IV tumors compared with nontransformers. Similarly, model estimates showed a significantly higher proliferation ($p = 0.0324$) and invasion rate ($p = 0.0050$) in WHO II–IV tumors compared with nontransformers. **Conclusion:** Tumor growth kinetics can identify contrast-enhancing diffuse astrocytomas undergoing malignant transformation.

[1]Harvard Medical School, 25 Shattuck Street, Boston, MA 02115, USA
[2]Department of Radiological Sciences, David Geffen School of Medicine, University of California, Los Angeles, 924 Westwood Boulevard, Suite 615, Los Angeles, CA 90024, USA
[3]UCLA Neuro-Oncology Program, David Geffen School of Medicine, University of California, Los Angeles, CA 90095, USA
[4]Department of Neurology, David Geffen School of Medicine, University of California, Los Angeles, CA 90095, USA
[5]Department of Biomedical Physics, David Geffen School of Medicine, University of California, Los Angeles, CA 90095, USA
[6]Department of Bioengineering, Henry Samueli School of Engineering & Applied Science, University of California Los Angeles, Los Angeles, CA 90095, USA
*Author for correspondence: Tel.: +310 481 7572; Fax: +310 794 8657; bellingson@mednet.ucla.edu

Future Medicine part of fsg

KEYWORDS
• glioma growth model • growth rate • low-grade gliomas • malignant transformation • MRI

Low-grade diffuse astrocytomas constitute a significant number of newly diagnosed primary brain tumors each year [1]; however, prognosis and clinical management of diffuse astrocytomas varies widely and there is currently no consensus as to how, or when, diffuse astrocytomas should be treated. Because of the relatively benign behavior and slow growth, many clinicians believe there is insufficient evidence to justify aggressive treatment for all diffuse astrocytomas [2], since many treatments can lead to substantial toxicity issues and morbidities. Other clinicians argue that treatment of all diffuse astrocytomas may prevent malignant transformation (i.e., transformation of diffuse astrocytomas to malignant tumors such as glioblastoma [GBM]) [3]; yet, there is little evidence for worsened outcome when treatment is deferred [4]. Contrast-enhancing diffuse astrocytomas are an aggressive subtype that represent approximately 34% of all low-grade astrocytomas and have shorter overall and progression-free survival compared with nonenhancing low-grade astrocytomas [5]. Despite being an aggressive phenotype, however, many contrast-enhancing low-grade astrocytomas remain WHO II even after recurrence and can also remain relatively indolent for months to years. Because contrast-enhancing diffuse astrocytomas are an understudied patient population with increased risk of tumor recurrence and few radiographic indications for transitioning to higher grade, there is a need for development of noninvasive tools that can quantify risk of malignant transformation to optimize clinical management strategies.

Currently, clinicians rely on relatively subjective assessment of serial MRIs to get a broad sense of aggressivity based on how fast a low-grade tumor appears to be growing over time. Brain tumor growth characteristics are traditionally estimated by volumetry, or segmentation of the tumor region of interest at each follow-up time point and calculating the rate of change in volume per unit time. A recent study by Rees *et al.* [6] demonstrated that simple estimates of tumor volumes and growth rates can provide more reliable and early insight into whether a particular low-grade glioma will undergo malignant transformation. Specifically, investigators noted that low-grade gliomas that eventually transform to higher grades have faster tumor growth rates from the time of diagnosis, and within 6 months of tumor progression there was acceleration of these growth rates. Therefore, we hypothesized that a more sophisticated biomathematical model of glioma growth and invasion may also provide insight into whether diffuse astrocytomas are undergoing malignant transformation. In particular, we hypothesize that growth kinetics estimated using a spatiotemporal glioma growth model of tumor cell density as a function of both space and time [7–9] may better predict malignant transformation, since this model has been shown to provide valuable patient-specific information used to predict response to therapy [10–13] and there have been few applications of this model to low-grade gliomas [14,15]. Thus, the purpose of the current study was to explore whether tumor growth kinetics estimated using a biomathematical model of tumor growth and invasion applied to serial MRIs could stratify contrast-enhancing low-grade diffuse astrocytomas patients that undergo malignant transformation to higher grades at the time of suspected tumor recurrence.

Methods

• Biomathematical model of tumor growth & invasion

A biomathematical model of tumor growth and invasion was previously described using a reaction–diffusion partial differential equation, quantifying cell density as a function of both space and time [7–9]. This model is derived from a more generalized mass–balance equation, in which the total number of tumor cells in a specific location can increase by either tumor cells migrating into this region or by tumor cells proliferating. Mathematically, this can be described as:

Rate of change in cell density

$$\frac{\delta}{dt}c(x,t) =$$

Cell invasion | Cell proliferation

$$= \nabla \cdot (D\nabla c(x,t)) + \rho \cdot c(x,t)\left(1 - \frac{c(x,t)}{K}\right)$$

where c(x,t) is the tumor cell density (cells/mm^3) as a function of both position, x, and time, t; D is tumor cell motility or diffusion (mm^2/year); ρ is tumor proliferation rate (year $^{-1}$); and

$$\rho \cdot c(x,t)\left(1 - \frac{c(x,t)}{K}\right)$$

is a logistic tumor growth term governed by the tissue cell carrying capacity, K (cells/mm^3). Previous investigators have also shown that the asymptotic estimate of the rate of radial growth of the tumor (i.e., velocity of the growing tumor wavefront) over long growth times can be estimated using Fisher's approximation [9,10,12]:

$$v = 2\sqrt{D\rho}$$

Consistent with the methods outlined previously by other groups, regions of contrast enhancement on postcontrast T1-weighted images and T2 hyperintense regions on T2-weighted or fluid-attenuated inversion recovery (FLAIR) images were assumed to represent 80 and 16% of the carrying capacity (i.e., 0.8 K and 0.16 K), respectively **(Figure 1)** [12]. The velocity of radial growth of the tumor can be calculated by analyzing serial imaging (as few as two) for an individual patient, then using Fisher's approximation estimates of $D \cdot \rho$ can be determined. Additionally, the T1-weighted and T2/FLAIR images from a single day can be used to infer the gradient of tumor cell density, given the approximation to the carrying capacity noted above. This gradient is related to the 'invisibility index', D/ρ, which combined with Fisher's approximation allows for direct estimation of D and ρ, as outlined previously. [7,9,12,13].

• Patients

A total of 30 patients with newly diagnosed low-grade (WHO II) diffuse astrocytomas that underwent tumor progression followed by surgical resection with at least two sequential contrast-enhancing MRI scans (one scan at the time of recurrence and one scan just prior to recurrence) undergoing no therapy at the time of recurrence were retrospectively identified in the UCLA Neuro-Oncology Database between January 2005 and January 2013. (Note: contrast enhancement is required for analysis and 34% of low-grade diffuse astrocytomas have contrast enhancement). Of these 30 patients, 14 patients did not progress to a higher tumor grade (WHO II–NT, or nontransformers), eight patients transformed to anaplastic astrocytomas (WHO II–III) and eight patients transformed to GBM (WHO II–IV) via histology. The average interval between these two MRI scans for all patients was approximately 304 days (range was 54–2112 days between scans) and the average interval did not differ between patient groups (ANOVA, p = 0.4499; WHO II–NT = 228 days, WHO II–III = 453 days, WHO II–IV = 288 days). Data acquisition were performed in compliance with all applicable regulations of the Health Insurance Portability and Accountability Act. All UCLA patients in this study signed institutional review board-approved informed consent to have their data included in our research database.

• Magnetic resonance imaging

Standard anatomical MRIs were acquired by using either a 1.5T (Signa Excite HDxt GE Medical Systems, Waukesha, WI; Sonata or Avanto, Siemens Healthcare, Erlangen, Germany) or 3T MR system (Trio, Verio or Skyra, Siemens, Erlangen, Germany). Scan sessions included at least the minimum required for implementation in the mathematical model, or precontrast and postcontrast (gadopentetate dimeglumine, Magnevist; Berlex, Wayne, New Jersey; 0.1 mmol/kg) axial T1-weighted fast spin echo images with matched scan parameters along with T2-weighted fast spin echo and/or FLAIR images. All images were acquired using pulse sequences supplied by the manufacturer.

• Tumor segmentation & volume estimation

Contrast-enhancing and T2-weighted hyperintense tumor regions were segmented by using standard techniques. Briefly, postcontrast T1-weighted and either T2-weighted or FLAIR images were Z-score Gaussian intensity normalized (i.e., images were zero meaned and scaled by the whole brain standard deviation of imaging intensities) and tumor areas were isolated by thresholding the images based on a z-score value. Final segmentations were manually edited to exclude nontumor or erroneous tissues. A spherical approximation to the resulting tumor volume, V, was used to estimate the radius of tumor on both postcontrast T1-weighted and either T2-weighted or FLAIR images using the formula:

$$r = \sqrt[3]{\frac{3V}{4\pi}}$$

This procedure was repeated for both recurrence scans and for scans just prior to recurrence.

• Definition of disease progresssion

Progression was defined prospectively by the treating neuro-oncologists if subsequent scans

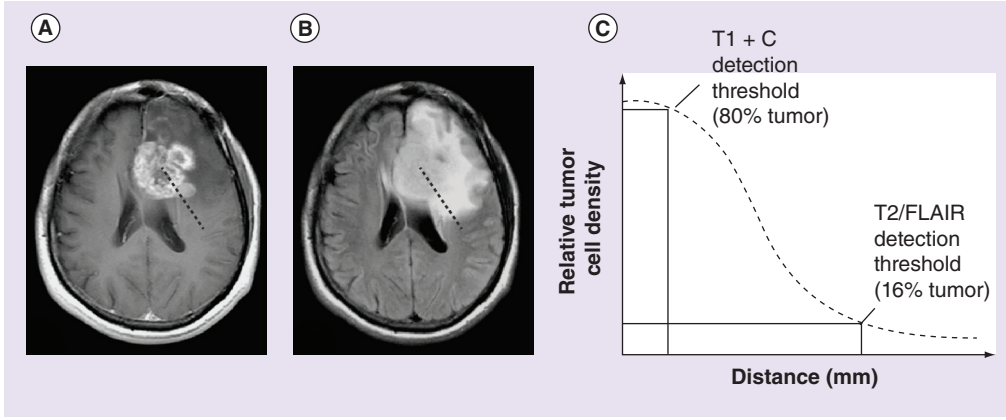

Figure 1. Estimation of relative tumor cell density for use in the mathematical model using anatomic MRI scans. A line drawn from the center of the tumor toward the periphery on **(A)** contrast-enhancing tumor on postcontrast T1-weighted images and **(B)** T2 hyperintense regions on T2-weighted or FLAIR images depicts areas of high and low cell density, respectively. As shown in **(C)**, the edge of the contrast-enhancing tumor is used to describe the isocellularity line at 80% of the tissue carrying capacity while the edge of the T2 hyperintense lesion describes the isocellularity line at 16% of the tissue carrying capacity. These measurements are used to estimate the gradient of cell density across the brain.
FLAIR: Fluid-attenuated inversion recovery.

showed an increase in imaging-evaluable tumor (≥25% increase in the sum of enhancing lesions, new enhancing lesions >1 cm^2, an unequivocal qualitative increase in nonenhancing tumor or an unequivocal new area of noncontrast-enhancing tumor). Additionally, patients requiring increased dosage of steroids in order to maintain neurologic function, even in the absence of worsening on anatomical images, were considered to be stable, but required early reevaluation. Patients who experienced significant neurologic decline were also declared to have progressed at the time of irreversible decline.

• Hypothesis testing & statistical analysis

Because radial expansion, invasion and proliferation rates were not normally distributed, a nonparametric Kruskal–Wallis test was performed to examine differences across patient groups (WHO II–NT; WHO II–III and WHO II–IV). Dunn's test was performed to examine individual differences in radial expansion, invasion and proliferation rates between groups. A p-value of less than 0.05 was considered significant after adjusting for multiple comparisons. Additionally, a receiver-operator curve (ROC) analysis was performed to determine the ability for radial expansion, invasion or growth rates to predict tumors that will undergo malignant transformation at the time of recurrence. The area under the ROC curve (AUC) was used as a metric of ROC performance.

Results

Consistent with our hypotheses and previous observations, patients with contrast-enhancing diffuse astrocytomas demonstrated changes in tumor size over time that appeared to increase with increasing malignancy. For example, patients with contrast-enhancing low-grade astrocytomas at the time of recurrence that did not transform into higher grade tumors (WHO II–NT) showed only small changes in tumor size when compared with the scans prior to recurrence (Figure 2A–D), whereas patients with diffuse astrocytomas that transformed to anaplastic astrocytomas (WHO II–III) at recurrence showed slightly more tumor growth compared with nontransformers (Figure 2E–H). Additionally, patients with diffuse astrocytomas that transformed to GBM (WHO II–IV) at the time of recurrence showed very rapid, dramatic changes in their tumor size when examining the scans leading up to recurrence (Figure 2I–L).

A closer examination of simple diffuse astrocytoma growth measurements during tumor recurrence substantiated these general observations. In particular, results suggested a significant difference in the rate of radial expansion in the contrast-enhancing portion of the tumor

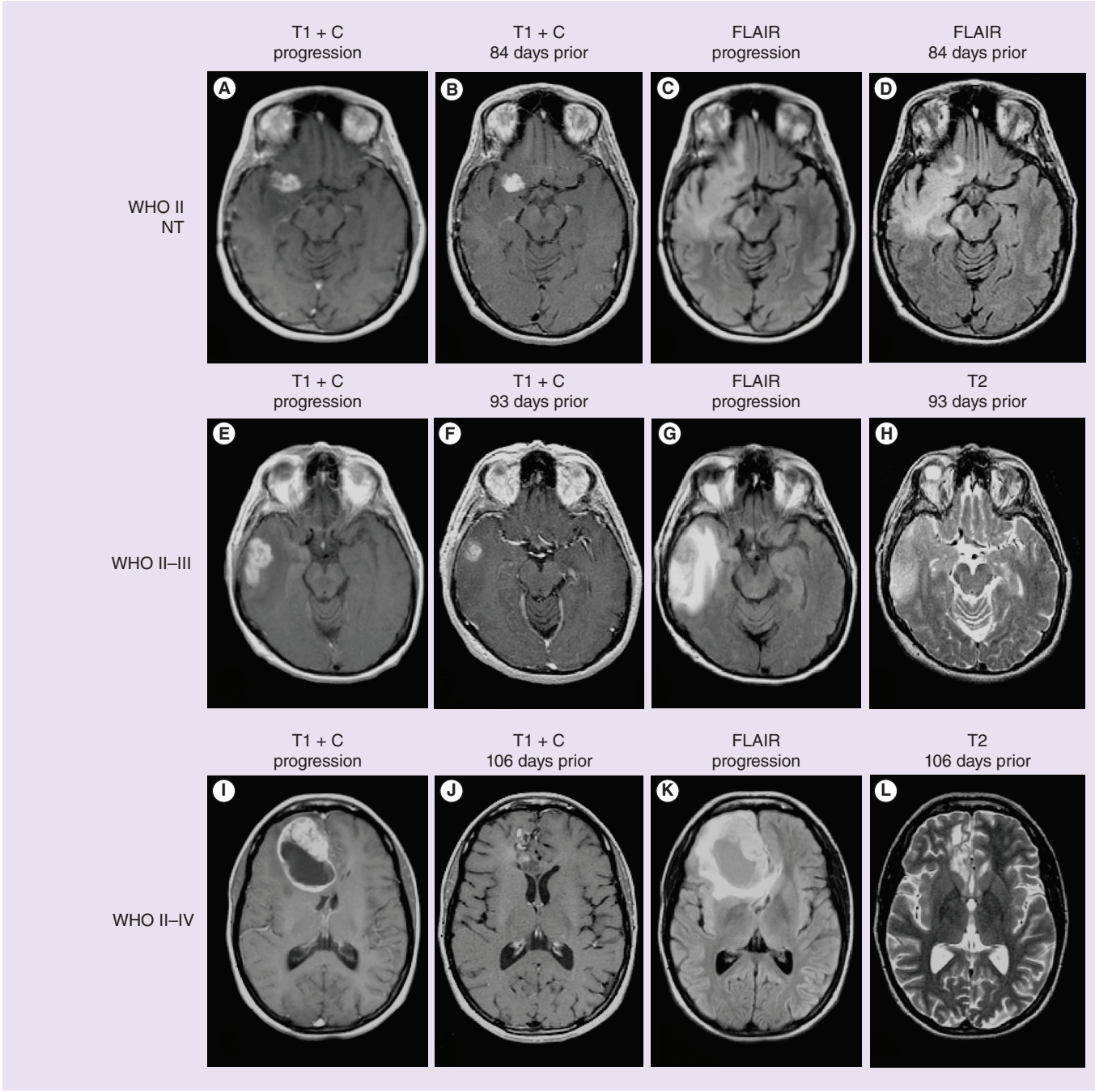

Figure 2. Examples of contrast-enhancing diffuse astrocytomas. **(A–D)** WHO II diffuse astrocytomas that did not transform (nontransforming). **(A)** Postcontrast T1-weighted image at radiographic progression. **(B)** Postcontrast T1-weighted image at previous imaging time point, 84 days prior to progression. **(C)** T2-weighted FLAIR image at radiographic progression. **(D)** T2-weighted FLAIR image 84 days prior to progression. **(E–H)** WHO II diffuse astrocytomas that transformed to WHO III anaplastic astrocytomas. **(E)** Postcontrast T1-weighted image at radiographic progression and malignant transformation. **(F)** Postcontrast T1-weighted image at previous time point, 93 days prior to radiographic progression. **(G)** T2-weighted FLAIR image at the time of progression and malignant transformation. **(H)** T2-weighted image 93 days prior to radiographic progression and malignant transformation. **(I–L)** WHO II diffuse astrocytomas that transformed to WHO IV glioblastoma. **(I)** Postcontrast T1-weighted image at radiographic progression and malignant transformation to glioblastoma. **(J)** Postcontrast T1-weighted image 106 days prior to recurrence and malignant transformation. **(K)** T2-weighted FLAIR images at progression and **(L)** T2-weighted image 106 days prior to recurrence and transformation.
FLAIR: Fluid-attenuated inversion recovery; NT: Nontransforming.

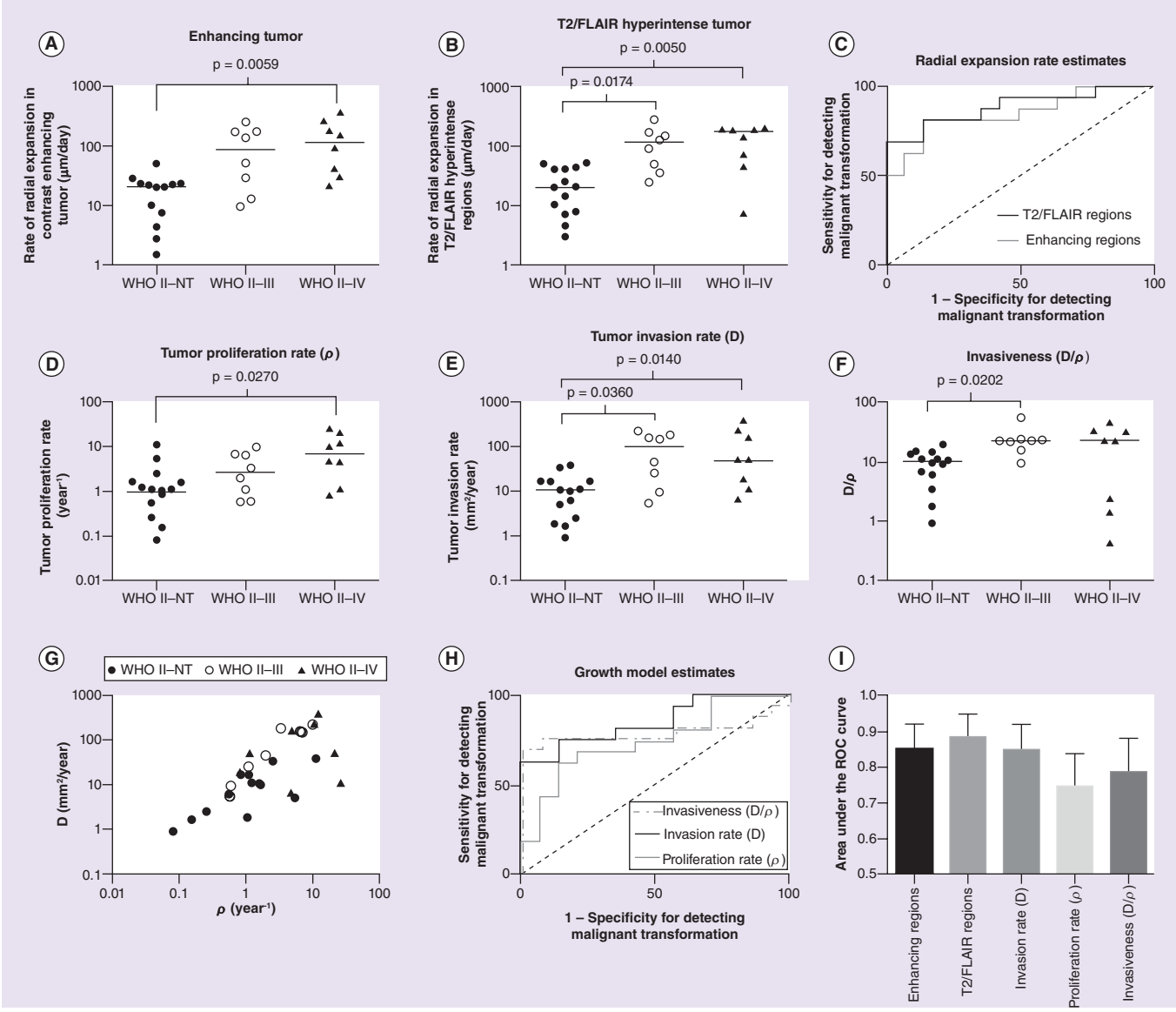

Figure 3. Radial expansion rates and glioma growth kinetics in contrast-enhancing diffuse astrocytomas. (A) Rate of radial expansion of contrast-enhancing tumor (in µm/day) showing a significantly higher expansion rate in diffuse astrocytomas that transform to glioblastoma (WHO II–IV) compared with nontransformers (Dunn's test, adjusted p = 0.0059). **(B)** Rate of radial expansion of T2/FLAIR hyperintense tumor showing a significantly higher expansion rate in diffuse astrocytomas that transform to anaplastic astrocytoma (WHO II–III; Dunn's test, adjusted p = 0.0174) or glioblastoma (WHO II–IV; Dunn's test, adjusted p = 0.0050) compared with NT. **(C)** ROC curves showing the rate of radial expansion for contrast-enhancing (AUC = 0.85 ± 0.07, p = 0.0012) and T2 hyperintense tumor (AUC = 0.88 ± 0.06, p = 0.0004) could both identify tumors undergoing malignant transformation (WHO II–III or WHO II–IV) from NT. **(D)** Tumor proliferation rate estimated from the mathematical model showed significantly higher rates in diffuse astrocytomas that transformed to anaplastic astrocytomas compared with NT (WHO II–III; Dunn's test, adjusted p = 0.0270). **(E)** Tumor invasion rate showed a significantly higher rate in diffuse astroctyomas that transform to anaplastic astrocytoma (WHO II–III; Dunn's test, adjusted p = 0.0360) or glioblastoma (WHO II–IV; Dunn's test, adjusted p = 0.0140) compared with NT. **(F)** The 'invasiveness', or the ratio of D/ρ, was significantly different between diffuse astrocytomas undergoing transformation to anaplastic astrocytomas (WHO II–III; Dunn's test, adjusted p = 0.0202). **(G)** Log–log plot of diffuse astroctyoma growth characteristics, showing proliferation and invasion rates for both nontransformers and transformers. **(H)** ROC curves for invasion rate (AUC = 0.85 ± 0.07, p = 0.0012), proliferation rate (AUC = 0.75 ± 0.09, p = 0.0222) and invasiveness ratio (AUC = 0.79 ± 0.09, p = 0.0078). **(I)** Comparison of the area under the ROC curve (AUC) showing slightly higher performance when using the radial expansion rates of T2/FLAIR hyperintense tumor regions than other measures of tumor growth and expansion.

FLAIR: Fluid-attenuated inversion recovery; NT: Nontransforming; ROC: Receiver-operator characteristic.

(Figure 3A) (Kruskal–Wallis, p = 0.0040) with tumors that degenerated into GBM showing a significantly higher rate of expansion compared with those that did not transform (Dunn's test, adjusted p = 0.0059). A measured rate of radial expansion of enhancing tumor more than 29 um/day during tumor progression had a sensitivity of 81% and specificity of 86% for identifying tumors that transformed to high-grade astrocytomas (Figure 3C) (ROC analysis, AUC = 0.85 ± 0.07 standard error of the mean, p = 0.0012). Similarly, the rate of radial expansion in the T2/FLAIR hyperintense regions of the tumor also showed significant differences among patient groups (Figure 3B) (Kruskal–Wallis, p = 0.0016). Multiple comparisons testing confirmed that nontransforming diffuse astrocytomas had significantly lower rates of T2/FLAIR radial expansion compared with both tumors that recurred as anaplastic astrocytomas (WHO II–III; Dunn's test, adjusted p = 0.0174) as well as those that transformed to GBM (WHO II–IV; Dunn's test, adjusted p = 0.0050). Similar to radial expansion rates of enhancing tumor regions, radial expansion rates of T2/FLAIR hyperintense regions higher than 45 um/day during progression showed an 82% sensitivity and 86% specificity of identifying diffuse astrocytomas undergoing malignant transformation (ROC analysis, AUC = 0.88 ± 0.06, p = 0.0004).

Mathematical modeling estimates of tumor motility and proliferation rates derived from radial expansion rate measurements showed similar trends to T2/FLAIR and contrast-enhancing radial expansion rates, respectively. Estimates of proliferation rate, ρ, varied significantly by patient group (Figure 3D) (Kruskal–Wallis, p = 0.0324), for which proliferation rate during tumor progression was higher in low-grade astrocytomas that transformed to GBM (WHO II–IV; Dunn's test, adjusted p = 0.027) but no difference was observed between nontransformers and tumors that recurred as anaplastic astrocytomas. The average proliferation rates were 2.06 $year^{-1}$ for nontransformers, 3.87 $year^{-1}$ for WHO II–III transformers and 10.22 $year^{-1}$ for WHO II–IV transformers. An estimated proliferation rate more than 3 $year^{-1}$ showed a sensitivity of 63% and specificity of 86% of identifying malignant transformation (Figure 3F) (ROC Analysis, AUC = 0.75 ± 0.09, p = 0.0222). Tumor invasion or motility rate, D, was also significantly different across patient groups (Figure 3E) (Kruskal–Wallis, p = 0.0050). The average tumor cell motility rate was 12.34 mm^2/year for nontransformers, 100.4 mm^2/year for WHO II–III transformers and 117.5 mm^2/year for WHO II–IV transformers. Similar to estimates of T2/FLAIR radial expansion rates, tumor invasion rates measured using the mathematical model varied significantly between nontransformers and both diffuse astrocytomas that transformed to anaplastic astrocytomas (WHO II–III; Dunn's test, adjusted p = 0.036) and those that transformed to GBM during progression (WHO II–IV; Dunn's test, adjusted p = 0.014). An invasion rate during tumor progression higher than 18 mm^2/year had a 75% sensitivity and 86% specificity of detecting malignant transformation (Figure 3H) (ROC Analysis, AUC = 0.85 ± 0.07, p = 0.0012). The ratio of invasion rate to proliferation rate, a measure of relative invasiveness of the tumor, was also significantly different across patient groups (Figure 3F) (Kruskal–Wallis, p = 0.0192), with significantly different measures of invasiveness between nontransformers and diffuse astrocytomas that recurred as anaplastic astrocytomas (Dunn's test, adjusted p = 0.0202). A ratio of D/ρ >15 had a sensitivity of 75% and specificity of 86% for identifying tumors that transformed to higher grade tumors during progression (Figure 3H) (ROC Analysis, AUC = 0.79 ± 0.09, p = 0.0078). No significant difference in the area under the ROC curve used to delineate nontransformers from diffuse astrocytomas that underwent malignant transformation at the time of progression was detected across any of the tumor growth metrics evaluated (Figure 3I) (ANOVA, p = 0.7387), but the rate of T2/FLAIR radial expansion showed the best performance. Despite similar performance, most of the metrics demonstrated high specificity but low sensitivity for identifying malignant transformation.

Discussion

Unlike GBM (WHO IV), low-grade diffuse astrocytomas (WHO II) can typically be controlled with standard therapy for many years; however, the precise timing and type of therapies are still controversial. During routine follow-up or therapy, many patients lead normal lives with nearly intact baseline neurological function. The ability to control diffuse astrocytomas as a chronic disease, however, is usually abruptly interrupted by the development of malignant transformation. Malignant transformation is functionally defined as occurring when a glioma increases in histological grade; however,

this remains a poorly understood process by which gliomas somehow acquire more aggressive features ultimately leading to death from rapid and uncontrolled tumor growth. There is tremendous variability in the reported likelihood of malignant transformation, ranging anywhere from 35 to 89% of tumors evaluated [16–18]. The threat posed by malignant transformation is amplified by the fact that transformation usually occurs without apparent warning even in patients that may have been stable for many years. Prevention and early identification of malignant transformation, therefore, is very important to provide the best hope of improving survival in patients with low-grade diffuse astrocytomas.

Results from the current study suggest that malignant transformation in contrast-enhancing diffuse astrocytomas result in a rapid expansion of contrast-enhancing and T2 or FLAIR hyperintense regions. Both rapid radial expansion rates as well as elevated estimates of growth and invasion rates obtained using the glioma growth model identified tumors undergoing malignant transformation with a high specificity, but relatively low sensitivity, when evaluated during the duration of tumor progression. Although beyond the scope of the current study, the rates of change and whether the tumors undergo malignant transformation also appeared to correlate with the pattern of enhancement. Complimentary to the study Pallud *et al.* [19], we noticed that more nodular tumors tended to have higher growth rates and higher rates of malignant transformation compared with both ring enhancing and patchier or faintly enhancing tumors, suggesting the pattern of contrast enhancement may also provide important insight into brain tumor behavior.

Consistent with the recent report from Rees *et al.* [6], simple estimates of radial expansion rates appeared to be able to identify tumors undergoing malignant transformation. Interestingly, radial expansion rates performed slightly better than more sophisticated measurements obtained using the glioma growth model. ROC analysis also confirmed this observation, showing slightly higher performance in T2/FLAIR radial expansion rates compared with all other metrics. This suggests estimates of tumor expansion rates on both contrast-enhanced T1-weighted and T2 or FLAIR images may be sufficient for quickly identifying contrast-enhancing diffuse astrocytomas at risk for progressing to a more aggressive tumor type. However, different combinations of D and ρ can result in similar measures of radial expansion; therefore, more sophisticated measures of tumor growth rates may provide additional information beyond that of expansion velocities.

• Limitations

There are a number of limitations that should be addressed in the current study. First, evaluation of growth kinetics using the diffusion-reaction relies on there to be measurable contrast enhancement at all time points during the evaluation. Since the majority of diffuse astrocytomas are nonenhancing because they typically lack histological features of vascular proliferation, evaluation is limited to contrast-enhancing low-grade astroctyomaas using the current mathematical model. Another potential limitation in the current study is the assumption that complex growth characteristics can be estimated from relatively simple measurements on MRI scans at two time points. In the current study we focused on the use of two sequential MRI scans leading up to the time of recurrence in order to determine whether malignant transformation can be identified; however, previous studies using this model chose to use two arbitrary time points during therapy. Additionally, the current mathematical model does not account for the regular use of corticosteroids, which can alter the amount of edema and contrast enhancement observed on MRI scans. Similarly, the current model is limited in that it assumes that T2/FLAIR hyperintense regions contains a specific amount of infiltrating tumor, which is not always the case. Areas of well-circumscribed nonenhancing tumor can have relatively high cellularity and high proliferation rates, whereas other regions of extending vasogenic edema can have a very low concentration of tumor cells. Regions of contrast enhancement do not always contain the highest density of tumor cells, as contrast enhancement can have mixed proportions of dense, proliferating tumor as well as increased vascular permeability from treatment-related effects such as radionecrosis or pseudoprogression. Further, regions of necrotic tumor growth are not explicitly represented in the growth model, which constitutes another limitation of the current model. Additionally, due to the retrospective nature of the study, molecular characteristics including IDH1 mutation and MGMT methylation status were not known but likely played a significant role in

prognosis and response to therapy. Lastly, the currently implemented model based on previous methodology [7,9,12,13] uses spherical approximations to estimate the radial expansion rates by first quantifying the volume of tumor from MRI scans. The conversion from volumetric to radial expansion estimates can introduce errors as the true tumor geometry deviates from spherical geometry (i.e., higher surface area to volume of the tumor).

Conclusion

Diffuse astrocytomas are diverse and heterogeneous types of tumors with significant variability in growth characteristics and survival times. This heterogeneity of biological behavior has led to a diverse range of opinions on optimal treatment strategies. Decisions regarding when to proceed with surgery, whether biopsy or resection, and when to use radiation or chemotherapies all remain areas of active debate [20]. Given the lack of definitive data regarding the best treatment options and the myriad of treatment approaches available, information about tumor growth characteristics may be valuable for personalized tumor management in diffuse astrocytoma.

Future perspective

Results from the current study suggest simple measures of radial expansion may be useful for predicting patients that will undergo malignant transformation. This information may be useful in future clinical practice for early identification of low-grade glioma patients at high risk for malignant transformation, for which more aggressive treatment may be necessary.

Financial & competing interests disclosure

Grant support: NIH/NCI R21CA167354 (BME); UCLA Institute for Molecular Medicine Seed Grant (BME); UCLA Radiology Exploratory Research Grant (BME); University of California Cancer Research Coordinating Committee Grant (BME); ACRIN Young Investigator Initiative Grant (BME); Art of the Brain (TFC); Ziering Family Foundation in memory of Sigi Ziering (TFC); Singleton Family Foundation (TFC); Clarence Klein Fund for Neuro-Oncology (TFC). The authors have no other relevant affiliations or financial involvement with any organization or entity with a financial interest in or financial conflict with the subject matter or materials discussed in the manuscript apart from those disclosed.

No writing assistance was utilized in the production of this manuscript.

References

Papers of special note have been highlighted as:
• of interest

1 Ostrom QT, Gittleman H, Farah P *et al.* CBTRUS statistical report: primary brain and central nervous system tumors diagnosed in the United States in 2006-2010. *Neuro Oncol.* 15(Suppl. 2), ii1–ii56 (2013).

2 Cairncross JG, Laperriere NJ. Low-grade glioma. To treat or not to treat? *Arch. Neurol.* 46(11), 1238–1239 (1989).

3 Yordanova YN, Moritz-Gasser S, Duffau H. Awake surgery for WHO grade gliomas within "noneloquent" areas in the left dominant hemisphere: toward a "supratotal" resection. Clinical article. *J. Neurosurg.* 115(2), 232–239 (2011).

4 Recht LD, Lew R, Smith TW. Suspected low-grade glioma: is deferring treatment safe? *Ann. Neurol.* 31(4), 431–436 (1992).

5 Chaichana KL, McGirt MJ, Niranjan A, Olivi A, Burger PC, Quinones-Hinojosa A. Prognostic significance of contrast-enhancing low-grade gliomas in adults and a review of the literature. *Neurol. Res.* 31(9), 931–939 (2009).

6 Rees J, Watt H, Jager HR *et al.* Volumes and growth rates of untreated adult low-grade gliomas indicate risk of early malignant transformation. *Eur. J. Radiol.* 72(1), 54–64 (2009).

• **Similar study examining the role of volumetric and radial growth rates in predicting malignant transformation in low-grade gliomas.**

7 Harpold HL, Alvord EC Jr, Swanson KR. The evolution of mathematical modeling of glioma proliferation and invasion. *J. Neuropathol. Exp. Neurol.* 66(1), 1–9 (2007).

• **Describes the use of a biomathematical model of glioma proliferation and invasion used in the current study.**

8 Tracqui P, Cruywagen GC, Woodward DE, Bartoo GT, Murray JD, Alvord EC Jr. A mathematical model of glioma growth: the effect of chemotherapy on spatio-temporal growth. *Cell Prolif.* 28(1), 17–31 (1995).

9 Wang CH, Rockhill JK, Mrugala M *et al.* Prognostic significance of growth kinetics in newly diagnosed glioblastomas revealed by combining serial imaging with a novel biomathematical model. *Cancer Res.* 69(23), 9133–9140 (2009).

10 Rockne R, Rockhill JK, Mrugala M *et al.* Predicting the efficacy of radiotherapy in individual glioblastoma patients *in vivo*: a mathematical modeling approach. *Phys. Med. Biol.* 55(12), 3271–3285 (2010).

11 Rockne R, Alvord EC Jr, Rockhill JK, Swanson KR. A mathematical model for brain tumor response to radiation therapy. *J. Math. Biol.* 58(4–5), 561–578 (2009).

12 Corwin D, Holdsworth C, Rockne RC *et al.* Toward patient-specific, biologically optimized radiation therapy plans for the treatment of glioblastoma. *PLoS ONE* 8(11), e79115 (2013).

13 Swanson KR, Rostomily RC, Alvord EC Jr. A mathematical modelling tool for predicting survival of individual patients following resection of glioblastoma: a proof of principle. *Br. J. Cancer* 98(1), 113–119 (2008).

14 Mandonnet E, Pallud J, Clatz O *et al.* Computational modeling of the WHO grade II glioma dynamics: principles and applications to management paradigm. *Neurosurg. Rev.* 31(3), 263–269 (2008).

15 Pallud J, Taillandier L, Capelle L *et al.* Quantitative morphological magnetic resonance imaging follow-up of low-grade glioma: a plea for systematic measurement of growth rates. *Neurosurgery* 71(3), 729–739; discussion 739–740 (2012).

16 Bobek-Billewicz B, Stasik-Pres G, Hebda A, Majchrzak K, Kaspera W, Jurkowski M.

Anaplastic transformation of low-grade gliomas (WHO II) on magnetic resonance imaging. *Folia Neuropathol.* 52(2), 128–140 (2014).

17 Philippon JH, Clemenceau SH, Fauchon FH, Foncin JF. Supratentorial low-grade astrocytomas in adults. *Neurosurgery* 32(4), 554–559 (1993).

18 Van Veelen ML, Avezaat CJ, Kros JM, Van Putten W, Vecht C. Supratentorial low grade astrocytoma: prognostic factors, dedifferentiation, and the issue of early versus late surgery. *J. Neurol. Neurosurg. Psychiatry* 64(5), 581–587 (1998).

19 Pallud J, Capelle L, Taillandier L *et al.* Prognostic significance of imaging contrast enhancement for WHO grade II gliomas. *Neuro Oncol.* 11(2), 176–182 (2009).

- **Describes the implications of contrast-enhancement patterns in malignant transformation.**

20 Schiff D, Brown PD, Giannini C. Outcome in adult low-grade glioma: the impact of prognostic factors and treatment. *Neurology* 69(13), 1366–1373 (2007).